Materials Today Electronics 1 (2022) 100003

Contents lists available at ScienceDirect

Materials Today Electronics

journal homepage: www.elsevier.com/locate/mtelec

Self-healing sensorized soft robots

Ellen Roels[a,*], Seppe Terryn[a], Joost Brancart[b], Fatemeh Sahraeeazartamar[b], Frank Clemens[c], Guy Van Assche[b], Bram Vanderborght[a]

[a] Brubotics, Vrije Universiteit Brussel and Imec, Pleinlaan 2, Elsene 1050, Belgium
[b] Physical Chemistry and Polymer Science (FYSC), Vrije Universiteit Brussel, Pleinlaan 2, Elsene 1050, Belgium
[c] Swiss Federal Laboratories for Materials Science and Technology (EMPA), Dübendorf, Switzerland

ARTICLE INFO

Keywords:
Sensors
Flexible electronics
Self-healing polymers
Soft robotics

ABSTRACT

The lifetime of soft robots is limited by their susceptibility to damage. Recent breakthroughs in healable soft robots have overcome this issue by manufacturing systems from self-healing polymers. However, to operate and recover autonomously, compatible sensors need to be embedded. We show that innovative healable soft sensors to measure strain, force, and damage, based on a self-healing conductive elastomeric composite, were developed and integrated with near-perfect interfacial strength in a healable soft gripper. The paper details the complete development of the gripper, including the selection of the conductive composite based on carbon black and nanoclay, sensor and actuator characterization, and its manufacturing. The gripper with embedded sensors recovers its actuation, sensor function, and damage detection after being severely damaged, and this multiple times.

1. Introduction

Soft robots, with their designs often inspired by nature, are currently under development for various applications, such as minimally invasive surgery [1], universal grasping [2] or locomotion on rough terrains [3], in which they often outperform their 'rigid' counterparts. Their inherent flexibility is key to their adaptability, enabling them to deform around obstacles. This gives them the advantage of being safe to work with humans and delicate objects. Their bodies usually consist of soft elastomers ($10^4 - 10^9$ Pa) [4], providing inherent flexibility. However, the soft behavior also makes them vulnerable to different types of damage [5]. Sharp objects [6], interfacial debonding [7], and fatigue [8] all pose a threat to soft robots, and limit their lifetime. Moreover, thermosetting elastomers are the main type of material used to manufacture soft robots and these are non-recyclable. The combination of a limited lifetime and a non-recyclability has led researchers to investigate various types of resilience [3,9]. A promising solution is to make these soft robots self healing. This can either be done by making smart use of materials [10], or by manufacturing them out of self-healing elastomers [11]. When damaged, these soft robots can heal, effectively prolonging their lifetime. However, not all self-healing polymers are suitable for use in soft robotics [5]. One type of self-healing mechanism that is deemed suitable are dynamic covalent bonds, like Diels–Alder (DA) based elastomeric networks [12]. When damaged, these polymers enable soft robots to heal upon mild heating (80–90 °C).

Recently, we have proven that DA materials that heal at room temperature can also be synthesized [13]. The choice for either an autonomous (room-temperature) or non-autonomous (mild heat) self-healing polymer depends largely on the application. Whereas autonomous healing needs no intervention other than recontacting the fracture surfaces, non-autonomous healing gives more control over the healing process, as the healing can be postponed and started whenever the temperature is increased (e.g., after re-alignment of shifted pieces) [13]. As they can be reprocessed and recycled, self-healing polymers also have an additional ecological advantage over traditional materials used in soft robotics, e.g., silicones [14,15].

Soft robots can bend, stretch, and twist around obstacles, which gives them the advantage of being safer, but the disadvantage of being harder to control due to their infinite degrees of freedom. Knowing the state of a soft system becomes almost impossible without proprioceptive sensors. However, in some applications, extensive control is less important and the robot does not always need to know its precise shape and state, as, in contrast to rigid robots, the morphology of soft robots takes care of a part of the computation [16]. It enables for example to grasp unknown objects without positioning the actuators exactly [2]. In many applications, morphological computation is not enough,

* Corresponding author.
E-mail addresses: ellen.roels@vub.be (E. Roels), seppe.terryn@vub.be (S. Terryn), joost.brancart@vub.be (J. Brancart), fatemeh.sahraeeazartamar@vub.be (F. Sahraeeazartamar), frank.clemens@empa.ch (F. Clemens), guy.van.assche@vub.be (G. Van Assche), bram.vanderborght@vub.be (B. Vanderborght).

https://doi.org/10.1016/j.mtelec.2022.100003
Received 2 March 2022; Received in revised form 6 May 2022; Accepted 1 June 2022
Available online 4 June 2022

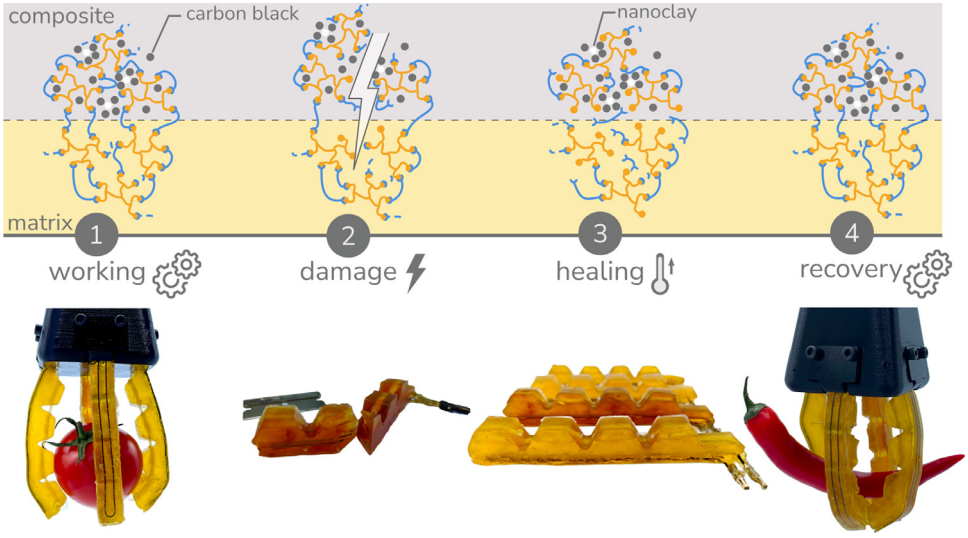

Fig. 1. Self-healing soft sensors are embedded in a soft self-healing gripper. The developed soft finger can fully heal from severe damage and the sensors can recover their sensing properties after damage.

and sensors are embedded to extend the capabilities of soft robots. For soft robots to continue benefiting from the advantages of their intrinsic flexibility, the embedded sensors need to be flexible as well. These deformation and force sensors enable the use of feedback motion control algorithms [17]. The sensors can be either proprioceptive (e.g., perceive whether its fingers are bent [18]) or exteroceptive, sensing the interaction with the environment (e.g., detection of an object in space [19,20]).

Creating sensors for soft robots remains challenging as the sensors should be soft, and can have only a limited influence on the mechanical properties of the actuator. Although flexible sensors have already been embedded in soft robotics to detect deformation and damage, they are, like the actuator in which they are embedded, vulnerable to damage [21–23]. This vulnerability is the motivation for the development of healable soft sensors made from self-healing materials like the DA based polymer networks [24]. Moreover, both for excellent sensor properties and robustness, the sensor and actuator materials should be compatible to enable a strong interface between both. This can be an issue for traditional elastomers where the interface between different materials mostly relies on weak physical interactions. Aside from introducing a healing ability, the reversible covalent bonds in the DA-based network enable the formation of strong (covalent) bonds across the multi-material interface, given that both materials are based on the same reversible chemistry [25,26]. This implies that not only the field of self-healing soft robotics sees great technological challenges in developing soft robots and their sensors, so does the field of material science. Novel elastomeric (composite) materials having a great potential for soft sensors used embedded conductive particles such as carbon (carbon black [27,28], carbon nanotubes [29–31]) and silver (nanowires (AgNW [32]), nanoparticles (AgNP) [33]). Also liquid metal [34,35], or intrinsically conductive materials can be used [36–38].

This work describes the development of innovative healable soft grippers with embedded sensors, in which all soft parts, including actuators as well as sensors, can recover from severe damage (Fig. 1). Both the conductive sensor material and the matrix material, in which this sensor is embedded, are self-healing. The four soft actuators show full recovery of mechanical and sensor properties after undergoing several modes of fatal damage. This approach does not only prolong the lifetime of the soft gripper, but it also removes the problem of delamination at the multi-material interface, a common cause of failure for soft robots [5]. As both the sensor and the surrounding matrix are self-healing and based on the same chemistry, they form a strong covalent interface, which is shown in Fig. 1. The whole development path from material to application is described. First, a conductive property is introduced in a self-healing polymer and its sensor properties are verified. The (non-conductive) DA polymers on which this work is based, have already proven their advantage in soft robots [12–14,25,26]. These materials are based on a thermo-reversible equilibrium reaction, often requiring mild heat to trigger and continue the healing process. To make these materials conductive and incorporate sensing properties, (hybrid) carbon black and nanoclay fillers were added. The influence of the filler content on the mechanical and healing properties is studied and discussed. The most promising composition is studied in detail and processed into different sensors by incorporating them into a non-conducting DA matrix material. We show that the interface between sensor and matrix material is nearly perfect, thanks to strong covalent bonds forming over the interface.

Two types of sensors are developed: piezoresistive strain sensors and capacitive touch sensors. Both piezoresistive sensors to measure strain [39], bending [40] and even force [41], and capacitive sensors to detect touch [42] or measure force [43] have already proven their use in soft robots. As will be shown, the developed sensors can recover their function and mechanical properties after fatal damage by subjecting them to a heat-cool cycle. Although studies have been published on healable sensors [24,44], to the authors' knowledge, most focus on the recovery of the electrical properties in unloaded conditions and in-depth analysis of the sensor property recovery is still lacking. The reason is that these healable soft sensors are difficult to model using analytical approaches due to their non-linear behavior and time-variant response. We show that the recovery of the actual sensory property is investigated in quasi-static and dynamic loading, based on the model of the sensory behavior.

First, we describe a thorough characterization of the developed material in Section 2. Afterwards, Section 3 does not only describe the characterization of the strain and touch sensor, but also provides the manufacturing process and the implementation in a healable soft gripper that recovers from fatal damage (see Fig. 1). Also on the actuator level, the recovery of the sensory behavior in cyclic operation is investigated in depth. The tendon-driven gripper is equipped with strain sensors that can measure the bending motion of the fingers as well as detect damage. These embedded sensors are soft, such that they do not compromise the flexibility of the soft gripper, preserving the adaptability and safety of the system.

2. Materials

2.1. Self-healing polymer

The self-healing property of the polymers used throughout this work, results from the Diels–Alder (DA) reaction between furan and maleimide functional groups, forming thermoreversible covalent crosslinks through the formation of two stereoisomeric DA adducts (called *exo* and *endo* isomers) [45]. The thermoreversible polymer network consists of the bismaleimide DPBM and the six-functional furan-functionalized Jeffamine FT5000. More details on the reagents and the synthesis can be found in supplementary information A. The DA reaction tends to a temperature-dependent equilibrium. The retro Diels–Alder reaction becomes increasingly important upon heating: the equilibrium shifts towards the reactants, DA bonds are progressively broken, and the mobility in the polymer network increases (Fig. 1). At the gel transition temperature (T_{gel}), extensive debonding leads to the degelation of the polymer network, and the elastomer is transformed into a viscous liquid oligomer melt, which can be (re)processed. When cooling down, the DA adducts are favored again, and crosslinks are reformed, eventually restoring the initial material properties. Upon mechanical damage, the DA bonds are broken preferentially, as these are the weakest covalent bonds in the network. The healing process starts by recontacting the fracture surfaces, which often occurs automatically by elastic recovery of the elastomer. Mildly increasing the temperature (e.g., to 80 °C) increases the mobility of the polymer network by reducing the crosslink density, and increases the number of reactive maleimide and furan groups, providing the mobility and reactivity required to seal and heal the damage (Fig. 1). When cooling down to room temperature (about 20 °C), the DA crosslinks are reformed throughout the network and across the fracture interface, restoring the full performance of the material. In theory, this enables the material to heal an infinite number of times at the same location. In practice, previous work has shown that the DA polymers have a healing efficiency of up to 98–99% per cycle, even after 30 thermal cycles [12].

By changing the network design parameters such as the monomer molecular weight, the stoichiometry of the reactive groups, and the monomer functionality, a wide range of material properties can be achieved and tuned to the requirements of the application [46]. The materials range from hard and brittle thermosets (Young's modulus $E \approx 1$–10 GPa) to soft and flexible elastomers ($E \approx 0.1$–100 MPa) suitable for an application in soft robotics. DPBM-FT5000-r0.5 was selected as the matrix material in which the sensor is embedded (Details in supplementary information A). Its hyperelastic mechanical properties ($E = 0.65 \pm 0.03$ MPa, fracture stress of 0.37 ± 0.02 MPa, fracture strain of $184 \pm 14\%$) make it an ideal candidate to be applied in soft robotics. This material was therefore used to manufacture the tendon-driven actuators in the soft grippers (yellow material in Fig. 1). Due to the lower maleimide/furan stoichiometric ratio r of 0.5, the crosslink density is lower than in a stoichiometric system, resulting in higher segmental chain mobility, and in an excess of furan groups that accelerates the DA reaction kinetics, which enables this material to heal at room temperature and recover from damage within a few minutes up to a week, depending on the location and magnitude of the damage [13]. The healing can be sped up further by subjecting the polymer network to a heat treatment. For healing robotic parts, the healing temperature should be kept below the T_{gel} to ensure mechanical stability of the polymer network and the retention of the 3D structure of the sensor and soft robotic actuator. The T_{gel} determined using dynamic rheometry is 95 °C (see supplementary information A). Healing tests (Fig. 2F) at a temperature of 80 °C for 40 min on samples that were cut in half and brought back in contact, show that the material reaches an average healing efficiency of 96% based on fracture stress. For the entire strain window, the hyperelastic relationship between stress and strain is regained, illustrating an excellent recovery of the mechanical properties.

2.2. Electrically conductive self-healing composites

To produce healable sensors for soft robotics, a conductive self-healing material is required that not only recovers its mechanical performance, but also its electrical and sensor properties. By adding carbon black (ENSACO 260G, Imerys, noted as CB260) as a conductive filler to a DPBM-FT5000-r0.6 material, an electrically conducting self-healing elastomer with a stoichiometric maleimide/furan ratio r of 0.6 was prepared. Different filler loadings were used to evaluate the effect of the presence of the filler on the viscoelastic and mechanical properties, and on the electrical conductivity of the formed composites. The elastic modulus of the composites increases with filler loading, while the electrical conductivity shows a percolation threshold, as the conductivity sharply increases by almost four orders of magnitude from 25 to 30 wt.% of carbon black in Fig. 2A. According to literature, the optimal piezoresistive sensor response is found in composites right above the percolation threshold [47,48]. Therefore, the composite with 30 wt.% carbon black is the most promising based on these results.

The incorporation of carbon black into the self-healing polymer matrix has a stiffening effect on the mechanical properties. All compositions were tested in two healing conditions, both at room temperature and 80 °C or 90 °C. Room temperature healing is not feasible for these materials (see supplementary information A). Unfortunately, with healing efficiencies all below 60%, even when heating, none of the materials reaches a satisfactory level of healing. The presence of high loadings of carbon black drastically reduces the segmental mobility of the polymer chains, which negatively impacts the healing behavior.

Nanoclay To overcome this issue, a small amount (1 wt.%) of an organomodified nanoclay (Cloisite 15A, Southern Clay Products Inc., noted as C15A) was added to the composite formulations. The addition of nanoclay has been described in the literature to result in a haloing effect, where the carbon black particles are no longer homogeneously dispersed in the matrix, but form a halo around the nanoclay [49], leading to an increase in conductivity and a shift in the percolation threshold. We observed a similar effect at higher CB filler loadings by the addition of a small amount of nanoclay. The percolation threshold can be observed as the sudden increase of electrical conductivity of several orders of magnitude from about 10^{-2} to 10^{2} S m^{-1}. Fig. 2A shows that the composites with 1 wt.% nanoclay all have a higher conductivity for the same carbon black load than those without nanoclay. This results in a shift of the percolation threshold from 25–30 wt.% to 15–20 wt.%. The composite with 20 wt.% carbon black and 1 wt.% nanoclay was selected as the new candidate to manufacture self-healing sensors, having a conductivity similar to the composite with 30 wt.% carbon black. Furthermore, the material with hybrid filler shows an improved healing efficiency (based on fracture stress) of 98% when heated to 90 °C for 1 h (see Fig. 2H). Therefore, this composite is deemed suitable to make sensors and is the one used throughout this study.

2.3. Interface

Having confirmed the healing ability of the matrix and the conductive composite individually, the interface between the non-conductive and conductive self-healing elastomers is investigated. High interfacial strength at multi-material connections is of high importance for creating sustainable multi-material soft robots which are robust to delamination. Excellent bonding between sensor and matrix, also increases the sensitivity of the sensor, as the sensor follows the deformation of the soft robot in which the sensor is embedded. The matrix polymer (DPBM-FT5000-r0.5) is based on the same DA chemistry as the conductive composite (DPBM-FT5000-r0.6 + 20 wt.% CB260 + 1 wt.% C15A) and, the two materials can thus be joined via covalent bonds using a heat-cool cycle. To illustrate this, multi-material samples were prepared where both networks were joined by subjecting them to a heat-cool cycle at selected temperatures, below their T_{gel} to preserve the shape of the specimens.

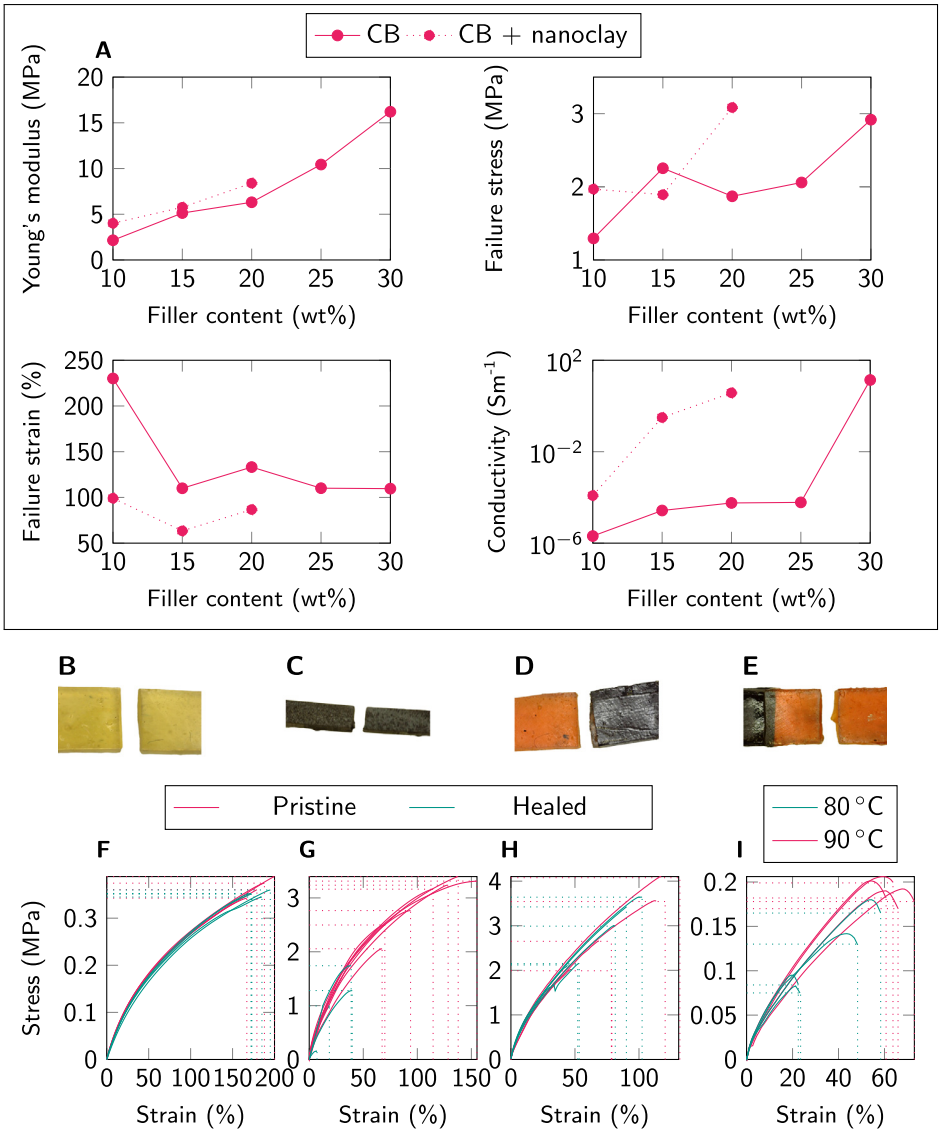

Fig. 2. Material properties of DA polymer composites. (**A**) Properties of materials filled with carbon black and a combination of carbon black and 1 wt.% C15A. (**B–E**) Images of the fracture zone of different samples: (B) unfilled polymer matrix, (C) 20 wt.% carbon black and 1 wt.% nanoclay, (D) fracture at interface between matrix and composite for parts joined at 80 °C, (E) fracture not at interface between matrix and composite for parts joined at 90 °C. (**F–I**) Tensile healing tests of DA polymers: (F) unfilled polymer matrix, (G) 30 wt.% carbon black, (H) 20 wt.% carbon black and 1 wt.% nanoclay, (I) samples of the matrix connected to the composite show a stronger interface when connected at 90 °C instead of 80 °C.

By raising the temperature, gradually thermoreversible bonds break that can be reformed across the interface between the two materials (Fig. 1). Moreover, at higher temperatures, the chemical reaction kinetics become faster, leading to a faster and more effective connection across the interface.

For healing and fusing purposes, it has to be taken into account that the neat polymer matrix and the conductive composite show different rheological behavior. The slightly higher stoichiometric ratio of the composite leads to a gel transition temperature T_{gel} of 105 °C, whereas that of the neat matrix material is 95 °C (see supplementary information A). The healing temperature should be kept below the lowest T_{gel} to ensure that both materials keep their mechanical stability. Samples were fused at 80 °C or 90 °C, for 45 min. After cooling down and waiting for at least 24 h, each sample was strained at a rate of 60% min^{-1} until failure. Fig. 2I shows that the samples fused at 90 °C do not only fail at higher strains, they also do not fail at the interface between the two materials, while the samples fused at 80 °C failed at the interface (see Fig. 2D and E). This indicates a near-perfect bond formed at 90 °C, one that is stronger than the weakest of the two materials, *i.e.* the neat polymer matrix, as was the case in previous work [25]. A good interface enhances the sensor response as it avoids unwanted interactions [50].

3. Results

3.1. Self-healing strain sensor

Combining the self-healing polymer and the self-healing electrically conducting composites, a self-healing strain sensor was developed. Numerous types of soft strain sensors exist based on different geometries [21]. For this first demonstration of the self-healing sensor technology, a simple strain sensor geometry was selected: a straight conductive fiber integrated into a non-conductive insulating matrix (Fig. 3A). A thin sensor fiber provides good conductivity without stiffening the matrix material and the soft robot in which this material is embedded, such that the sensor is nearly mechanically invisible to the system.

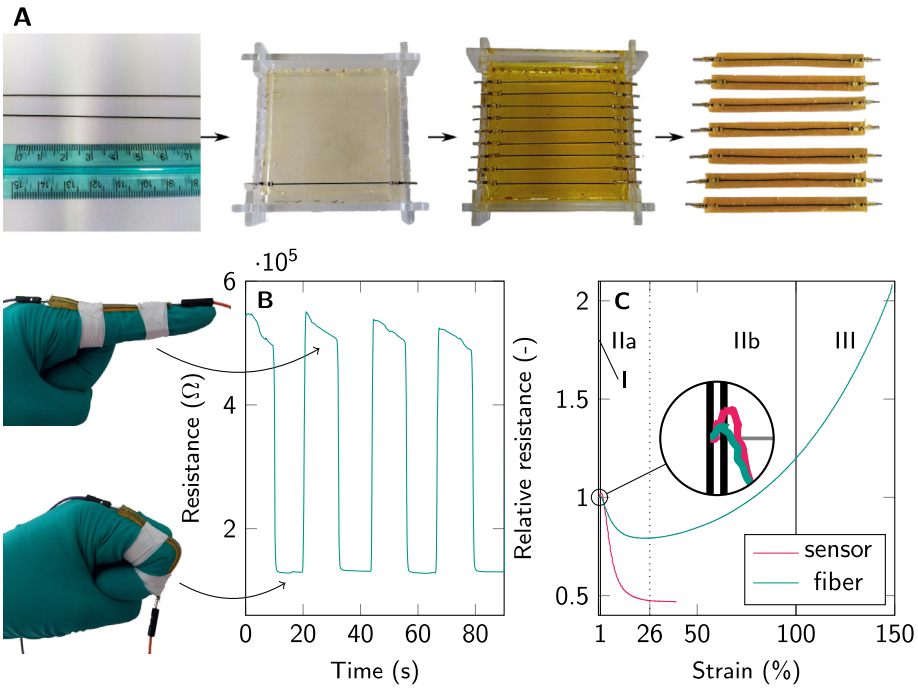

Fig. 3. Manufacturing and characterization of the self-healing strain sensor. (**A**) Self-healing conductive fibers are embedded in a matrix of self-healing DA polymer using a mold enabling fiber alignment. The fiber ends are fitted with crimp connectors to ensure a good electrical contact. The final strain sensors have a cross section of about 5 mm × 2.3 mm. (**B**) The sensor can be applied for human motion detection, it is attached to the dorsal side of the index finger. The sensor responds to repetitive bending and straightening of the index finger. (**C**) To analyze the sensor response, the fiber and sensor were strained at a rate of 10% min^{-1} while measuring their resistance. Four operating zones can be identified, zone IIa is chosen as the main operating zone for the sensor.

Straining the fiber changes its electrical resistance, from which the strain can be deduced. The conductive self-healing composite was extruded into fibers with a diameter (≈0.5 mm) using a customized piston extruder. Although in literature fibers with smaller diameters are used (e.g., 0.3 mm [27]), the choice of a larger diameter is a design consideration aimed at reducing the probability and impact of misalignment during the healing process. With such a fiber embedded in a non-conductive matrix material, not only the deformation can be measured, but it can also be determined whether the matrix or fiber is damaged [51], as damage that interrupts the current path will lead to a sharp increase in resistance. First, the different steps in the manufacturing process of the self-healing strain sensor will be elaborated. Next, the sensor will be characterized electrically and mechanically, before illustrating the recovery of these properties after the healing process of macroscopic damages.

3.1.1. Manufacturing of the strain sensor

The strain sensors are manufactured using a two-step process: fiber extrusion followed by embedding. First, the fibers are extruded in a custom-made piston extruder, equipped with temperature control and a 0.5 mm die. The extrusion is performed at 112 °C, above the T_{gel} of the composite. After resting at room temperature for at least 24 h, the fibers are ready to be used. The cross-section of the fiber was analyzed using scanning electron microscopy (SEM) to evaluate the diameter and roundness. A circular Hough transform (CHT) superimposes the optimal fitting circle on the image (see SH), the average ($n = 5$) diameter of the fiber is 498 μm, and the average resistance is 1726 ± 381 Ω/mm.

In the second step, the fibers are embedded in the insulating matrix polymer. The fibers are sandwiched between two layers of matrix material in a mold before the assembly is placed in an oven at 110 °C. At this temperature, the matrix starts to flow around the fibers, effectively encapsulating them. Although this temperature is above the T_{gel} of the composite, it retains its shape as no shear force is applied to the fiber. From the rheological data, it could be derived that the composite material retains predominantly solid-like behavior under small amplitude shear deformation, even above the gel transition temperature of the polymer, due to the presence of a percolating filler network (see supplementary information A). Only when sufficient shear force is applied to overcome the yield stress resulting from the physical filler network, the material shows a liquid-like flow behavior. The newly formed strain sensors were taken out of the oven and left to cool down at room temperature. After 24 h, they were removed from the mold and cut into separate sensors (more details in SB).

3.1.2. Electrical characterization

To investigate the relationship between strain and resistance, a composite fiber was subjected to a linearly increasing strain (10% min^{-1}), while the resistance was monitored using a Keysight E4980AL LCR meter on a dedicated test bench (more details in SE). The fiber was not embedded in the matrix, but only fitted with crimp connectors at both ends. Before electrical testing, the fiber was glued to cardboard on both ends to avoid damage due to the clamping force [52]. In the observed resistance-strain relationship presented in Fig. 3C four zones (I, IIa, IIb and III) are identified, corresponding to different regimes, as described by Flandin et al. and discussed in detail in SI [47].

As the resistance is important for the sensor, rather than the resistivity used by Flandin et al., zone II is split in two parts: IIa and IIb. The transition between both sub-zones is defined where the resistance is minimal. In zone IIa, the resistance decreases with increasing strain, whereas in zone IIb, it increases again to above the initial value. Zones I and III correspond to the initiation and recoverable damage zones as described by Flandin et al.

Looking at the resistance-strain relationship for the fiber presented in Fig. 3C, a surjection is observed for the entire strain interval, including the four zones: the same resistance value can be measured for multiple strain values. This however, is not problematic, when selecting a strain interval, e.g., zone IIa, as operating range. Although high strains are present in soft robotics upon actuation (e.g., 100% for pneumatic sys-

tems [12]), these are often localized, while soft strain sensors are mostly integrated in sections in which the strains are more limited (<30%). Thus, in this paper, zone IIa was selected as operating strain window for the strain sensor, as the relation between resistance and strain requires a bijection (a one-to-one relation) to keep the sensor readout straightforward. When the sensor fiber breaks, the resistance becomes infinite and the fiber can thus be used for rudimentary damage detection.

After characterizing the resistance-strain behavior of the fiber, the embedded fibers were characterized as well. Fig. 3C shows the same test done for a strain sensor (a fiber embedded in the matrix) strained until 40%. Zones I and IIa are shown, the latter corresponding to the operating range. The matrix material also influences the sensory behavior, as described by Georgopoulou et al. [50].

The sensitivity of the fiber and sensor can be derived based on the gauge factor (GF), a widely used characteristic of (piezoresistive) strain sensors. This dimensionless number is determined using the formula:

$$GF = \frac{\Delta R/R_0}{\varepsilon} \tag{1}$$

with resistance R, initial resistance R_0, and strain ε. However, this relationship can only be used to reconstruct the strain from the resistance when the response is approximately linear. The sensors developed in this work have an overall non-linear strain-resistance response, which renders the GF useless for reconstruction purposes. However, it remains useful as a way of comparing with the sensitivity of sensors presented in literature. Fig. 4E shows again that the resistance starts to increase slightly at strains above 26%. Because determining a single GF over the domain 0%-30% has no meaning, two gauge factors were determined using the 'broken stick regression' approach. The break point divides the domain in two parts and is calculated such that the angle between both linear regressions is maximal. The gauge factors are calculated by taking the average over the last 10 cycles of the test, as the sensor is then in steady state. For the pure fibers, the break point was determined at 11% strain with GF equal to 3.2 ± 0.4 and 0.15 ± 0.02. For the sensors where this fiber is embedded in, the break point lies at 10 ± 2% strain, and the GF amounts to 7.2 ± 1.3 and 0.26 ± 0.03 ($n = 9$), respectively, in the two domains. Even though the second GF is on the lower end of the spectrum, the values correspond to common GF values found in literature for elastomeric sensors (typically $10^0 - 10^2$) [53]. It also shows that embedding the fibers in the matrix had a positive effect on their sensor properties.

Soft strain sensors are promising for smart robotic wearables, including artificial skins and smart gloves, used for health and performance monitoring or as haptic devices. Although the human skin can withstand strains up to 150% [54], the strains during normal functioning are limited. This is illustrated by a first feasibility study, in which the self-healing strain sensor was affixed to the dorsal side of the index finger of a test subject (Fig. 3B). Upon folding and straightening the sensor cyclically, the resistance responds. The resistance drops each time the sensor bends (the fiber stretches) and increases again when it is straightened, which verifies that the sensor operates in zone IIa in this application. Zone IIb can also be used in soft robotics or wearables, when the sensor is integrated in sections that are subjected to high strains (30%), or by pre-straining the fiber before embedding it in the matrix. Although pre-straining fibers for strain sensors is commonly done [50], the reversible nature of the DA crosslinks in these self-healing elastomers would over time relax this pre-strain, leading to a sensor whose characteristics would undesirably evolve in time.

A cyclic measurement gives more insight in the dynamic behavior of the strain sensor. The strain sensors were subjected to a sinusoidal strain with strain amplitude of 15%, and a period of 10 s, for 100 cycles, on top of a static strain of 15%. All measurements are given in relative resistance, the average resistance of the sensors being 324 ± 66 kΩ ($n = 9$). Fig. 4E shows the relation between the relative resistance and the strain, which is an average response calculated over all cycles. Hysteresis, observed as loops in the dynamic response behavior, is a well-known phenomenon and common issue in resistive carbon black based sensors [53,55,56]. Both Fig. 4E and C, presenting the resistance-strain relation in loading and unloading, indicate that the hysteresis of the self-healing strain sensor is limited. However, Fig. 4A and C (data obtained from the same measurement) illustrate that the sensors exhibit non-negligible drift, probably caused by the viscoelastic relaxation of the DA polymer, which is also a well-known effect for similar polymers [57]. This slow relaxation can be illustrated by subjecting the elastomer to a square wave strain pattern (Fig. 4G). For the self-healing strain sensor embedded in an actuator of a gripper, this pattern could represent a cyclic grabbing, holding and releasing task. The sensor is repetitively strained to 20%, held, and released back to its initial length. Each position was held for 30 min. The resistance shows a slow relaxation of about 30% of the total change when moved back to its initial position, while it responds nearly instantaneously upon stretching. This relaxation was also observed when applying it for human finger motion detection in Fig. 3B. It results from the viscoelastic nature of the reversible polymer network, in combination with the 3D-network formed by the carbon black particles above the percolation threshold. A more detailed investigation of the relationship between the mechanical and electrical relaxation and the viscoelastic nature of the self-healing polymer networks and their composites is currently ongoing.

The observed time-dependent behavior makes it challenging to model the sensor analytically, solutions have thus been proposed to model soft polymeric sensors based on neural networks [17,58,59]. Although the development of a full analytical model is outside the scope of this work, we propose to fit a model on the sensor response when it approaches the steady state. For the cyclic measurements shown in Fig. 4A and B, a model is fitted based on the first half of the dataset, and applied to reconstruct the strain for the second half. First, the drift is removed from the resistance measurement by normalizing the data between the upper and lower enveloping curve. After the normalization, the graph $\varepsilon(R)$ is approximated with a second order rational function (1 zero, 2 poles) that is used for the reconstruction. When reconstructing the strain, it can be seen from Fig. 4G that the prediction accuracy is quite fair. Due to the drift of the sensors, this approach tends to slightly overestimate the strain over time. After 50 cycles, the maximal residual error is 7%. More details on this method are given in SJ.

3.1.3. Healing

We validated the self-healing performance of the sensor by studying the recovery of the mechanical and electrical properties of the embedded sensor. Two types of damage are distinguished, for which we investigated the healing. Cuts or tears can occur in the matrix in proximity to the sensor fiber, yet leaving the sensor fiber untouched (Type 1, Fig. 5A). Alternatively, more severe cuts can lead to damage of both the matrix and the sensor fiber (Type 2, Fig. 5B). In the latter case, the electrical properties of the sensor are severely affected and, ultimately, the resistance of the sensor will increase to infinity when severed completely. Both types of damage were induced using a scalpel blade. Two sensors were damaged by solely cutting the matrix (Type 1) and for six sensors also the sensor fiber was severed (Type 2). As Type 2 is the most severe damage situation, this type is better suited to verify the healing ability of the sensor, while also being the most challenging situation to recover both mechanical and electrical properties. One sensor was not damaged and was used as a reference.

Before initiating the healing procedure, the fracture surfaces of the sensor are recontacted and the fiber pieces should be aligned. Contact and alignment of the fiber was verified by measuring the resistance. Upon adequate contact, the resistance drops to a value within the same order of magnitude as the original value (10^5 Ω). The electrical signal can thus be used to assist alignment and healing in future applications. To

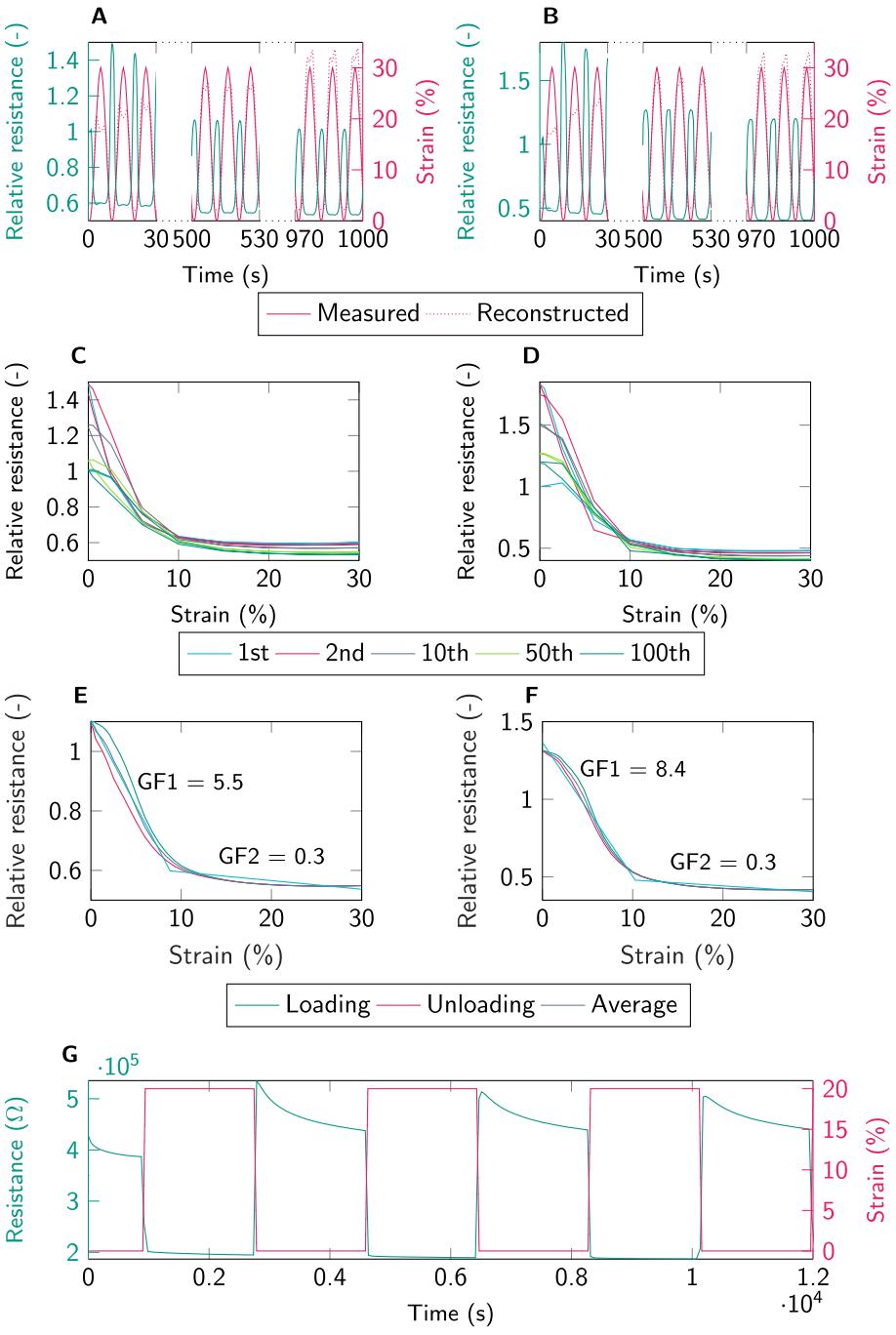

Fig. 4. Characterization of the self-healing strain sensor. (**A and B**) Time-based sensor response for a sensor strained with a sinusoidal load from 0% to 30% strain with a period of 10 s. (A) Pristine. (B) After healing. (**C and D**) Resistance versus strain response curves for different cycles. The sensor response drifts over time but shows little hysteresis. (C) Pristine. (D) After healing. (**E and F**) Averaged response curves for the last 10 cycles of the loading and unloading of one sensor following the same sinusoidal load. (E) Pristine. (F) After healing. (**G**) When subjected to a square wave strain pattern, the sensor shows a relaxation effect in the stretched state. The strain was changed between 0% and 20% at a rate of 30%/s, every step is held for 30 min.

illustrate this, two severely damaged sensors were healed after deliberately making insufficient contact and misalignment, whereas four were properly aligned and recontacted. All damaged sensors were healed by subjecting them to a temperature of 90 °C for 45 min. The reference sensor underwent the same temperature treatment. A bad contact (misalignment) leads to a value that is several orders of magnitude higher (10^7 Ω), even after healing. Microscope images illustrate (Fig. 5D) the small gap between the ends of the sensor fiber, causing the high increase in resistance.

The recovery of the sensor performance was investigated through the characterization of the healed sensors, using the same approach as before damage. All healed sensors show a similar response characteristic as before being damaged. In Fig. 4F, the average response cycle after healing is given for the healed sensors. For the two sensors that underwent damage type I, the gauge factors are 9.5 ± 0.56 and 0.37 ± 0.04, with the break point at 10% strain. For the four sensors for which the fiber was cut in two (type II), the gauge factors are now 12.9 ± 7.6 and 0.43 ± 0.13, with the break point at 11%. The GF of the sensors

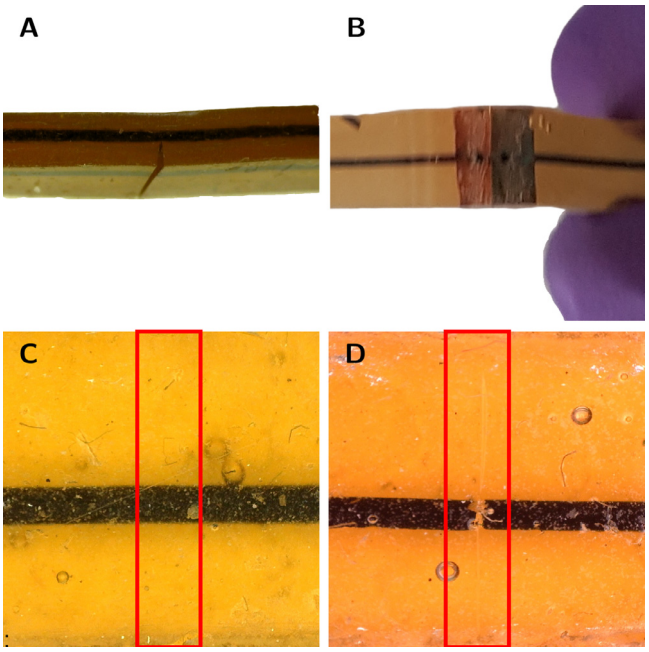

Fig. 5. Damage and healing of the strain sensor. (**A**) Damage type I of the sensor where only the matrix is cut. (**B**) Damage type II where both matrix and fiber are cut. For easier realignment the matrix was not cut completely. (**C** and **D**) Microscopic image of healed sensors. The damage location is indicated with a red rectangle. (**C**) Healed sensor after damage type II. (**D**) Sensor healed after an improper alignment, showing a gap between the two parts of the fiber. (For interpretation of the references to color in this figure legend, the reader is referred to the web version of this article.)

increased after this thermal treatment, which can also be seen for the reference sensor, where the GF increased from 6.7 and 0.29, to 9.2 and 0.36. This indicates that the sensor does not lose its sensitivity after healing, on the contrary, the sensitivity was increased, and that in a real application, a slight recalibration for the sensors would be required. Notwithstanding this, after healing severe damage, the sensors are healed well and recovered their original function.

3.2. Self-healing touch sensor

Soft grippers find major applications in agriculture, food, and collaborative manufacturing, in which they pick and place objects with various shapes and sizes, including fruits and vegetables [2]. When grasping, in many cases the robot requires feedback to determine whether it is touching or holding an object and the orientation of the object. This detection can be performed by a touch or force sensor, embedded in the flexible structure of the soft gripper [42,60]. Being soft and in contact with the surroundings, these touch sensors can, for example, be pierced by sharp objects, leading to failure of the sensor. Hence, a self-healing capacitive force sensor is proposed, entirely manufactured from self-healing polymers, which can recover from this type of damage.

3.2.1. Manufacturing

The proposed self-healing capacitive sensor consists of a sandwich structure, with two self-healing conductive layers (DPBM-FT5000-r0.6 + 20 wt.% CB260 + 1 wt.% C15A) separated by a self-healing dielectric layer (DPBM-FT5000-r0.5) (Fig. 6A). The sandwich is then encapsulated within non-conductive matrix material to isolate it. The conductive layers are manufactured using compression molding. These sheets are approximately 1 mm thick and have a protruding connection stem. The connection with the electronic is made using a crimp connector on each conductive layer. A third 0.5 mm thick layer of insulating DPBM-FT5000-r0.5 forms the dielectric between the plates. The sandwich structure is fused together via a heat treatment at 100 °C for 45 min to form a strong connection (SC describes the manufacturing process of the force sensor in more detail). The capacitance of this sensor can be approximated using the equation for an ideal parallel plate capacitor:

$$C = \frac{k\varepsilon_0 A}{d} \tag{2}$$

where $k\varepsilon_0 = 38.836$ pF/m is the storage permittivity of the dielectric material (DPBM-FT5000-r0.5 at 1 kHz, supplementary information A), $A = 314$ mm^2 the area of the plates, and $d \approx 0.5$ mm the distance between the plates. This results in a capacitance of 24 pF, which is quite close to 22.5 pF, the measured value of the sensor at rest.

3.2.2. Electrical characterization

A Keysight E4980AL LCR meter was used to measure the capacitance of the force sensor while a dedicated test setup (see SF) exerts a compression force on it. The LCR meter was calibrated both in open and short clamp configuration, and all measurements were performed at 1 kHz. The capacitance was measured as a function of the applied compression force using a dynamic load. A 0.1 Hz sinusoidal force was applied to the sensor, oscillating between 2.5 N and 7 N. Fig. 6C indicates that the sensor response is steady within consecutive cycles, but that a non-negligible drift is present when observing a larger timescale, which is again attributed to the dynamic character of the network. Fig. 6E shows the response for selected cycles, both in loading and unloading, indicating no notable hysteresis. The response is linear and the sensitivity can be expressed by following formula:

$$\text{sensitivity} = \frac{\Delta C}{\Delta F} \tag{3}$$

The obtained data result in a sensitivity of 0.027 pF/N, calculated on the 10th cycle.

A step response test enables to examine the relaxation behavior of the sensor response (Fig. 6I). When applying a 5 N static load, the sensor responds immediately, after which some relaxation and drift are noticeable. This is caused by the viscoelastic property of the DPBM-FT5000-r0.5 dielectric layer. The drift can be characterized as

$$\text{drift} = \frac{\Delta C}{C_{\max} \Delta t}$$

resulting in a value of 0.4%/h. Since the sensor exhibits a linear response behavior ($R^2 = 0.9919$, measured over the average of all cycles), the sensitivity can be used as a linear function to reconstruct the force from the capacitive measurement. The average sensitivity of the last 10 cycles were used to predict the next 100 cycles. As seen in Fig. 6G and discussed further in SK, the error of reconstruction is quite limited. The drift for this type of sensor is lower than for the self-healing strain sensor, and thus is the reconstruction valid over a larger timescale without sacrificing the precision of reconstruction.

3.2.3. Healing

To verify the healing of the touch sensor, a large cut was made through all layers of the sandwich structure, as shown in Fig. 6B. It has to be noted here that even if the sensor is completely cut in two, it does not lose its function as long as both connectors are on the same half. The area, and thus the capacitance, will be changed, but it will continue to work as a touch sensor. The damaged sensor was subjected to the same healing procedure as the strain sensors. It was heated at 90 °C for 45 min, before leaving it to rest for 24 h at room temperature. Fig. 6D, F, and J show that the self-healing sensor recovers its function after this damage-healing cycle, both in a dynamic and a step response test. The capacitance of the sensor has increased by about 3%, which can be due to stray capacitance from the environment, and the drift is now 0.8%/h. Comparing the 10th loading cycle, the sensitivity has barely changed from 0.027 pF/N to 0.032 pF/N, showing excellent recovery of the sensor behavior, even after these large cuts.

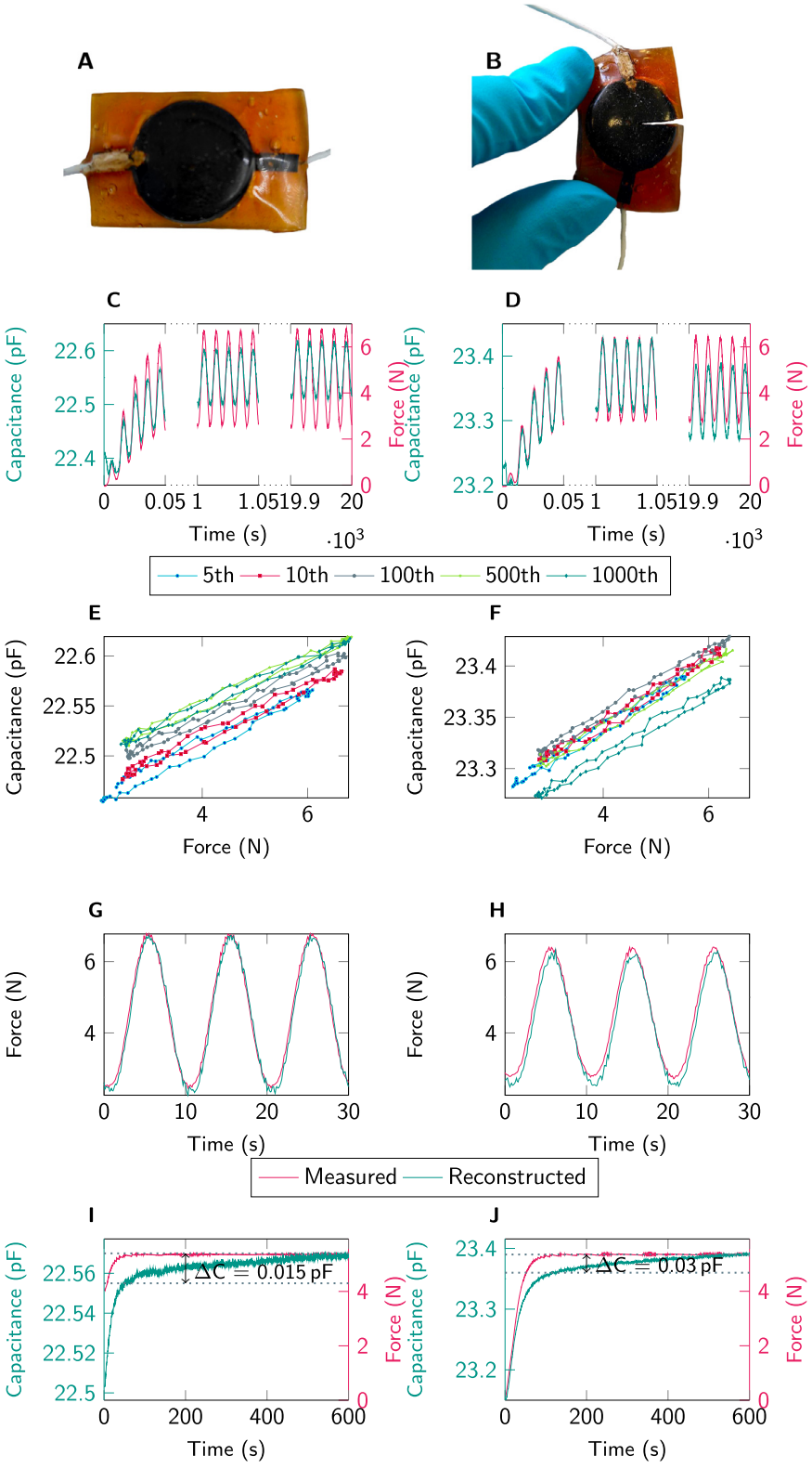

Fig. 6. Manufacturing and characterization of the capacitive touch sensor. (**A**) The pristine sensor. (**B**) Sensor damaged with a slit. (**C–F**) Time-based sensor response for 1000 cycles applied to the sensor at 0.1 Hz. After 100 cycles (1000 s), the sensor does not show apparent drift. The drift is however no longer negligible after 1000 cycles. Looking at the capacitance-force sensor response for individual cycles (E,F), the sensor does not show significant hysteresis and that the signal shows drift over time. (C,E) Pristine. (D,F) After healing, the sensor has recovered its properties. (**G and H**) By linearly fitting the sensor response, the force can be reconstructed based on the capacitance with low error. (H) Pristine. (G) After healing. (**I and J**) Response to a step-input. Data processed with a moving average window of 6. (I) The pristine sensor shows a drift of 0.015 pF after 10 min. (J) After healing, the sensor shows a drift of 0.03 pF after 10 min.

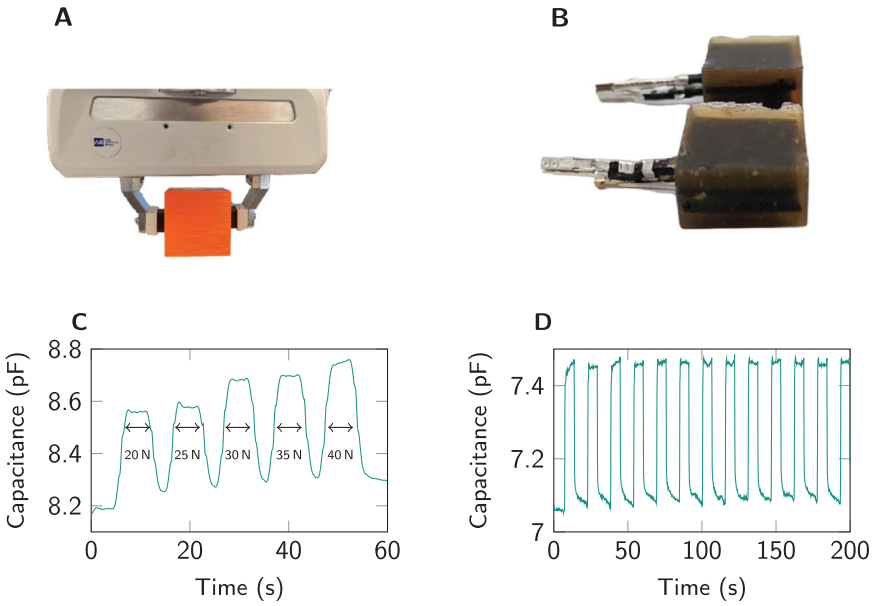

Fig. 7. Demonstration of the touch sensor in an industrial robot. (**A**) The gripper of the robot consists of two sliding fingers. The contact pads are replaced with touch sensors. (**B**) Close-up of the touch sensors that are used on the robot. (**C**) The robot is instructed to grasp a cube with increasing force. (**D**) The sensor shows no drift when repetitively grasping an object.

3.2.4. Implementation in an industrial robot

One of the touch sensors was implemented in the gripper of an industrial robot to show its potential. The gripper of the Franka Emika Panda robot consists of two sliding fingers with rubber contact pads (Fig. 7A). These contact pads ($\approx 1.5 \times 1.5$ cm^2) are replaced with self-healing touch sensors (Fig. 7B) placed in a 3D-printed holder to connect them to the fingers. The robot has an internal force sensor and is able to grasp objects with a force that can be set between 20 N and 100 N. This can be used to calibrate the sensor. The robot is instructed to grasp a $5 \times 5 \times 5$ cm^3 cube with increasing force (Fig. 7C). The object is grasped for 5 s, an released for another 5 s before grasping it again with more force. The sensor shows a clear increasing response. When the cube is grasped repetitively (grab 5 s, release 5 s) with a force of 20 N, the sensor shows a good response with no noticeable drift (Fig. 7D).

3.3. Self-healing gripper with embedded strain sensor

The concept of the strain sensor was validated by embedding it in a soft tendon-driven actuator, in which it acts as a bending sensor (Fig. 8A). By pulling the tendon, its length is shortened, and the actuator bends. The actuator consists of two parts that are compression molded separately: the phalanges structure and the backbone. As the backbone is on the outer side, and thus in tension while bending, this backbone is the ideal location to place the sensor. The sensor fiber is embedded in a U-shape to have both connectors at the base of the actuator. Both parts are fused at 80 °C for 30 min. More details on the manufacturing process of the actuator can be found in SD.

3.3.1. Characterization

The embedded strain sensor was characterized using an in-house developed set-up that consists of a tendon control system, a camera to measure the bending angle, and an LCR meter to record the resistance of the sensor. An in-depth explanation of the set-up is given in SG. During the characterization, the finger was kept horizontally at rest and bent upwards. The bending angle was defined as the angle between the horizontal resting position, and the line drawn through the base of the finger (where the finger is clamped) and the tip.

The finger reaches a maximal bending angle of 85 °when actuated, as shown in Fig. 8C. The sensor gives a good response, the resistance decreasing upon increasing bending, as it is located on the outer side of the finger and hence in tension. When looking at the resistance as a function of the bending angle during the same test, some hysteresis is noticeable. When not addressed in a real-world application, this might cause an issue. One possible solution is to use artificial intelligence to take the time dependence of the sensor into account. This is however considered outside the scope of the work presented here.

The finger was subjected to 100 actuation cycles up to the maximal bending angle. The sensor showed a good response to the bending, with limited drift over 100 cycles, as shown in Fig. 8E. Afterward, the finger was repeatedly subjected to various damage modes (Fig. 8G–I) and healed at 90 °C for 45 min. All three damages could be registered by the sensor as a sudden spike in resistance value toward infinite. This damage detection approach can be used in future soft robots, equipped with many embedded healable sensors, to detect large damages. The realignment of the fracture properties was performed manually but was assisted by tracking the resistance. Upon excellent alignment, the resistance reaches values in the same order of magnitude as the initial resistance at rest. The same bending tests were repeated after each damage-healing cycle. After recovering from the three types of damage shown, both the sensor and the finger fully recovered their function, as shown in Fig. 8F. After three damage-healing cycles, the sensor sensitivity is defined as

$$\text{sensitivity} = \frac{\Delta R/R_0}{\Delta \alpha}$$

decreased (based on the 10th cycle) from 0.0014 to 0.0012. Yet, this series of large damages could be healed, leading to a recovery of sensory properties, which could be used for tracking the bending angle after recalibration. Four of these fingers were combined in a self-healing sensorized gripper that can grasp objects of different sizes and shapes (see Fig. 8B).

4. Discussion

Self-healing polymers have found their way into soft robotics, where they can overcome a pressing issue: the vulnerability of these systems.

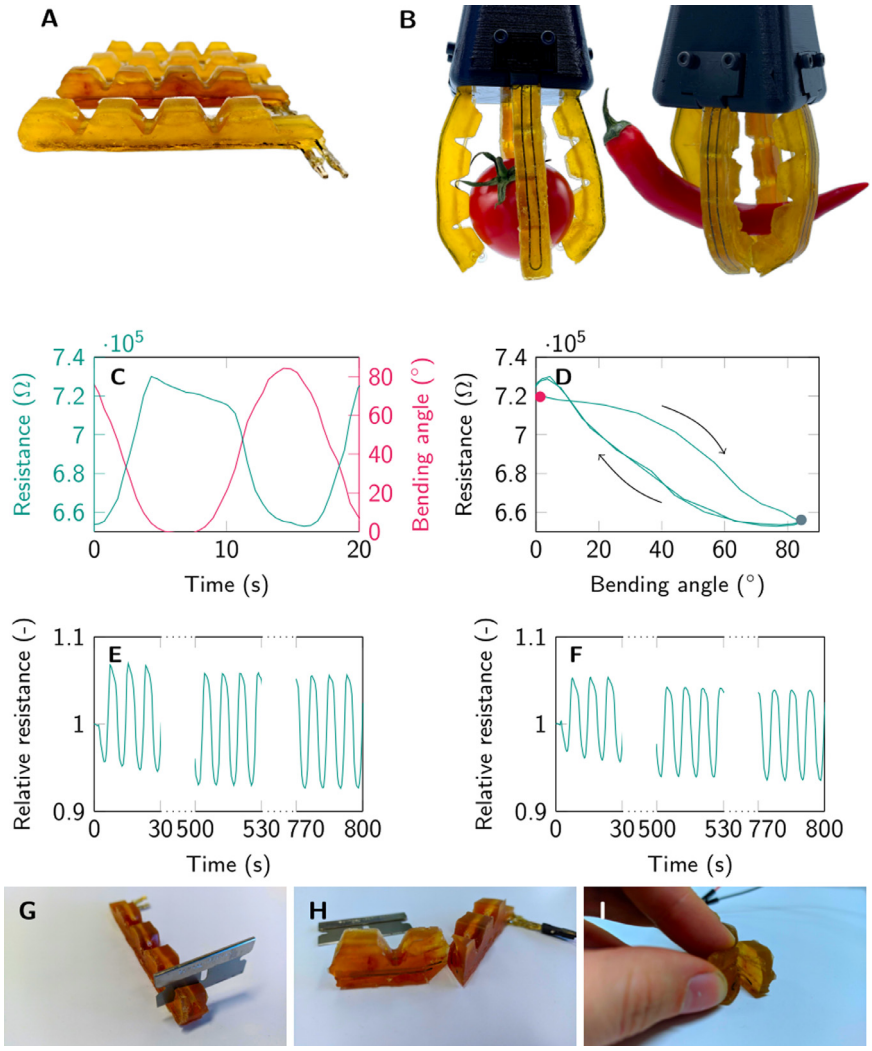

Fig. 8. Characterization of the finger. (**A**) A self-healing strain sensor is embedded in a soft tendon-driven finger. (**B**) Four fingers are combined into a gripper that can pick up different objects such as a tomato or a pepper. (**C**) The finger shows a good sensor response when bending. (**D**) When plotting the data from (**C**) as resistance in function of the bending angle (starting point in gray, end point in pink), some hysteresis is noticeable. (**E and F**) Cyclic tests of the actuator show limited sensor drift. (E) Pristine. (F) After three damage-healing cycles. (**G and I**) Different damages the actuator was subjected to.

Soft robots are quite susceptible to various modes of damage that occur in the soft elastomeric materials of which they are composed. Incorporating a healing property in these soft robots prolongs their lifetime, increasing their economical and ecological competitiveness in many future applications. Most materials used in soft robotics are thermosetting elastomers and can thus not be reprocessed, nor recycled. The self-healing Diels–Alder polymer chemistry used throughout this work has already proven its use in different types of robotic actuators and has shown to overcome these issues. Due to the reversible crosslinks in the polymer network, different damage types, including cuts, perforations, microcracks, and delamination, can be healed using heat treatment or fully autonomous at room temperature. Moreover, the reversible polymer network degels at high temperatures, resulting in a viscous liquid polymer. This liquid state enables reprocessing of the parts, further increasing the sustainability of future self-healing soft robots through recycling.

In many applications, the soft robot cannot be controlled without proprioceptive or exteroceptive integrated sensors. As these embedded sensors cannot compromise the compliance of the soft robotic system, soft polymeric sensors are mostly selected in the literature. In addition to the vulnerability of structural elements and actuators of a soft robot, also these soft sensors are vulnerable. Loss of these sensors through damage leads to systems with partial or complete functionality or efficiency losses. To overcome this vulnerability, we have successfully developed a fully self-healing actuator, with incorporated sensors, that can recover its mechanical function and sensing capacity, even after being completely sliced through. The healing property was incorporated into the actuators using a flexible Diels–Alder polymer network cross-linked with thermoreversible covalent bonds (DPBM-FT5000-r0.5). Electrical conductivity was obtained by introducing 20 wt.% of carbon black (Ensaco 260G) and 1 wt.% of nanoclay (Cloisite 15A) in the matrix material, DPBM-FT5000-r0.6, to obtain a conducting composite suitable for the sensors. Both the matrix and composite material have excellent mechanical properties, combining high strength with high strain, and excellent recovery of these mechanical properties after healing. A healing efficiency of 96% was achieved for the matrix, and 92% for the composite material. Both materials were used to make the self-healing sensorized robotic actuators. To the authors' knowledge, this is the first time that a sensorized robotic actuator is made, composed solely of materials that can all recover from large damages. The actuator can heal repeatedly by applying mild heat (90 °C) for 45 min, letting it cool down, and rest at room temperature for 24 h. After healing, the actuator and sensor performance is restored.

Excellent adhesion between sensor and matrix enhances the sensitivity of soft sensors and is often a critical point in resistive strain sensors, as load transfer is critical for strain sensing. By combining a Diels–Alder

composite and matrix, high interfacial strength is achieved between sensor and matrix, based on strong covalent bonds formed upon a heat-cool cycle. Hence, the use of self-healing polymers in soft sensors can contribute to the sensitivity. This adhesion was verified by fusing the matrix and composite materials at different temperatures. When a suitable fusing protocol is used, it was found that the weakest point where the samples failed, was no longer at the interface. This indicated a near-perfect chemical cohesion of the two materials, thanks to reversible covalent bonds being formed across their contact interface.

Two types of self-healing sensors were prepared with the conductive composite: a resistive strain sensor and a capacitive touch sensor. The sensing elements of both sensors were manufactured by shaping them above their gel temperature. The strain sensor employs a thin conducting composite fiber made using a piston extruder, while the capacitive sensor is based on thin disks of conducting and non-conducting self-healing materials prepared by compression molding. To be used as a strain sensor, the composite fiber requires good piezoelectric properties. We showed that the resistance decreases monotonously when strained between 1% and 26% and starts to increase again at higher strains. To limit the complexity of the sensor signal reconstruction, a sensor is preferably used in only one of the zones where the signal varies monotonously with the strain. For the sensors in this work, zone IIa was selected, where the resistance decreases with increasing strain. Although it limits the maximum strain, this is not necessarily a drawback, as this strain range corresponds to the range of strains usually seen in the field of soft robotics. The response of the self-healing capacitive touch sensor is based on the compression of the dielectric layer in between two conducting composite layers. Also, this sensor shows a good and linear response behavior when subjected to a load, with the capacitance decreasing upon compression. Both sensors show almost no hysteresis, but they have a non-negligible drift when subjected to a dynamic load. This drift is a known issue in many conductive elastomers, but can in this case also be attributed to the dynamic behavior of the Diels–Alder network. The relationship between electrical and mechanical relaxation in these self-healing composites will be studied further in future work.

The recovery of the sensor sensitivity after the damage was analyzed both on the sensor level as well as on the actuator level. In the prior art, the healing evaluation of soft sensors is mostly limited to the recovery of the electrical properties in unloaded conditions. However, to truly validate self-healing sensors, the recovery of the actual sensory behavior has to be investigated. This can only be performed based on a model of the sensor response of the flexible sensors. For both self-healing sensors made in this work, the resistive strain sensor and the capacitive force sensor, a broad quasistatic and dynamic characterization enabled to develop models for the sensor response, which were used to analyze the sensor recovery. For the capacitive force sensor, a linear relationship is suitable. Due to the drift of the strain sensors, a more complex approach is required, where the drift is taken into account and the resistance-strain behavior is fitted with a second-order rational. More advanced reconstruction approaches are out of the scope of this work, but they can be achieved using recent developments in artificial neural networks or by making an extensive model of the material. The first option is preferred, as it offers more flexibility to adapt when the properties change slightly after healing. For all sensors, the sensor response was recovered after healing large cuts, although small variations in sensitivity were detected. This means that recalibration of the sensors is required after healing. However, in many robotic systems, recalibrations are common and the authors still believe soft robotic applications will benefit economically from this healing capacity.

Aside from deformation and force sensing, the self-healing sensors can be used for damage tracking and healing evaluation as well. Large cuts and tears, that damage the sensor partially or completely cut through it, lead to abrupt high changes in resistance or capacitance which can be detected by the system. This damage detection can initiate healing, and is important to create healable soft robots in the future, capable of healing completely autonomous, without external intervention. It was also illustrated that tracking the sensor response upon recontacting the fracture surfaces, helps to reduce misalignment. Excellent recontact and minimal misalignment lead to sensor responses that are in the same order of magnitude as the original value. This data can therefore be used to help autonomous self-recontact in the future. Lastly, these sensors can be used to re-evaluate the health of the system, as the recovery of sensor properties enables to identify if recontact and healing were successful.

Although this field of self-healing sensors is accelerating fast, multiple challenges still need to be addressed, including reducing time-variant effects like drift and hysteresis in healable soft sensors and creating more robust models for simulating the complex non-linear and time-dependent sensor response using expanded analytical models or machine learning. Yet, the recovery of mechanical properties and sensor sensitivity at the sensor and actuator level, presented in this paper, illustrate the potential of the healing capacity. The authors believe that the self-healing materials, in particular the combination of Diels–Alder composites and polymers, can be an enabling technology for complex soft robotic systems with embedded sensors, including soft grippers, soft exoskeletons, and prosthetics, as the combination of healing and recycling capacity will lead to sustainable, economical long-life products.

Funding

This work was supported by the EU FET Open RIA Project SHERO (grant number 828818) and Fonds Wetenschappelijk onderzoek (grant number 1S84120N (ER), 1100416N (ST), 12W4719N (JB)).

Data and materials availability

All data is available on https://doi.org/10.5281/zenodo.5822474.

Declaration of Competing Interest

Authors declare that they have no conflict of interest.

CRediT authorship contribution statement

Ellen Roels: Conceptualization, Data curation, Formal analysis, Investigation, Software, Visualization, Writing – original draft. **Seppe Terryn:** Conceptualization, Investigation, Supervision, Writing – review & editing. **Joost Brancart:** Conceptualization, Investigation, Supervision, Writing – review & editing. **Fatemeh Sahraeeazartamar:** Formal analysis, Investigation, Writing – review & editing. **Frank Clemens:** Funding acquisition, Writing – review & editing. **Guy Van Assche:** Conceptualization, Funding acquisition, Project administration, Resources, Supervision, Writing – review & editing. **Bram Vanderborght:** Conceptualization, Funding acquisition, Project administration, Resources, Supervision, Writing – review & editing.

Supplementary material

Supplementary material associated with this article can be found, in the online version, at doi:10.1016/j.mtelec.2022.100003.

References

[1] B. Gorissen, M. De Volder, D. Reynaerts, Chip-on-tip endoscope incorporating a soft robotic pneumatic bending microactuator, Biomedical Microdevices 20 (3) (2018-09), doi:10.1007/s10544-018-0317-1.
[2] J. Amend, N. Cheng, S. Fakhouri, B. Culley, Soft Robotics Commercialization: Jamming Grippers from Research to Product, Soft Robotics 3 (4) (2016-12) 213–222, doi:10.1089/soro.2016.0021.
[3] M.T. Tolley, R.F. Shepherd, B. Mosadegh, K.C. Galloway, M. Wehner, M. Karpelson, R.J. Wood, G.M. Whitesides, A Resilient, Untethered Soft Robot, Soft Robotics 1 (3) (2014-09) 213–223, doi:10.1089/soro.2014.0008.

[4] D. Rus, M.T. Tolley, Design, fabrication and control of soft robots, Nature 521 (7553) (2015-05) 467–475, doi:10.1038/nature14543.

[5] S. Terryn, J. Langenbach, E. Roels, J. Brancart, C. Bakkali-Hassani, Q.-A. Poutrel, A. Georgopoulou, T. George Thuruthel, A. Safaei, P. Ferrentino, T. Sebastian, S. Norvez, F. Iida, A.W. Bosman, F. Tournilhac, F. Clemens, G. Van Assche, B. Vanderborght, A review on self-healing polymers for soft robotics, Materials Today (2021-03-20), doi:10.1016/j.mattod.2021.01.009.

[6] E. Cohen, V. Vikas, B. Trimmer, S. McCarthy, in: Design Methodologies for Soft-Material Robots Through Additive Manufacturing, From Prototyping to Locomotion, American Society of Mechanical Engineers Digital Collection, 2016-01-19, doi:10.1115/DETC2015-47507.

[7] Z. Wang, Y. Torigoe, S. Hirai, A Prestressed Soft Gripper: Design, Modeling, Fabrication, and Tests for Food Handling, IEEE Robotics and Automation Letters 2 (4) (2017-10) 1909–1916, doi:10.1109/LRA.2017.2714141.

[8] Y.S. Krieger, C.-M. Kuball, D. Rumschoettel, C. Dietz, J.H. Pfeiffer, D.B. Roppenecker, T.C. Lueth, Fatigue strength of laser sintered flexure hinge structures for soft robotic applications, in: 2017 IEEE/RSJ International Conference on Intelligent Robots and Systems (IROS), 2017-09, pp. 1230–1235, doi:10.1109/IROS.2017.8202297.

[9] R.A. Bilodeau, R.K. Kramer, Self-Healing and Damage Resilience for Soft Robotics: A Review, Frontiers in Robotics and AI 4 (2017), doi:10.3389/frobt.2017.00048.

[10] E. Acome, S.K. Mitchell, T.G. Morrissey, M.B. Emmett, C. Benjamin, M. King, M. Radakovitz, C. Keplinger, Hydraulically amplified self-healing electrostatic actuators with muscle-like performance, Science 359 (6371) (2018-01-05) 61–65, doi:10.1126/science.aao6139.

[11] T.-P. Huynh, P. Sonar, H. Haick, Advanced Materials for Use in Soft Self-Healing Devices, Advanced Materials 29 (19) (2017-05) 1604973, doi:10.1002/adma.201604973.

[12] S. Terryn, J. Brancart, D. Lefeber, G. Van Assche, B. Vanderborght, Self-healing soft pneumatic robots, Science Robotics 2 (9) (2017-08-16) eaan4268, doi:10.1126/scirobotics.aan4268.

[13] S. Terryn, J. Brancart, E. Roels, G.V. Assche, B. Vanderborght, Room Temperature Self-Healing in Soft Pneumatic Robotics: Autonomous Self-Healing in a Diels-Alder Polymer Network, IEEE Robotics Automation Magazine 27 (4) (2020-12) 44–55, doi:10.1109/MRA.2020.3024275.

[14] E. Roels, S. Terryn, J. Brancart, R. Verhelle, G. Van Assche, B. Vanderborght, Additive Manufacturing for Self-Healing Soft Robots, Soft Robotics 7 (6) (2020-03-10) 711–723, doi:10.1089/soro.2019.0081.

[15] E. Roels, S. Terryn, F. Iida, A.W. Bosman, S. Norvez, F. Clemens, G. Van Assche, B. Vanderborght, J. Brancart, Processing of Self-Healing Polymers for Soft Robotics, Advanced Materials 34 (1) (2022) 2104798, doi:10.1002/adma.202104798.

[16] C. Laschi, B. Mazzolai, Lessons from Animals and Plants: The Symbiosis of Morphological Computation and Soft Robotics, IEEE Robotics Automation Magazine 23 (3) (2016-09) 107–114, doi:10.1109/MRA.2016.2582726.

[17] T.G. Thuruthel, B. Shih, C. Laschi, M.T. Tolley, Soft robot perception using embedded soft sensors and recurrent neural networks, Science Robotics 4 (26) (2019) eaav1488, doi:10.1126/scirobotics.aav1488.

[18] J. Tapia, E. Knoop, M. Mutný, M.A. Otaduy, M. Bächer, MakeSense: Automated Sensor Design for Proprioceptive Soft Robots, Soft Robotics (2019-12-09), doi:10.1089/soro.2018.0162. soro.2018.0162

[19] J. Hughes, F. Iida, Tactile Sensing Applied to the Universal Gripper Using Conductive Thermoplastic Elastomer, Soft Robotics 5 (5) (2018-10) 512–526, doi:10.1089/soro.2017.0089.

[20] Y.-C. Lai, J. Deng, R. Liu, Y.-C. Hsiao, S.L. Zhang, W. Peng, H.-M. Wu, X. Wang, Z.L. Wang, Actively Perceiving and Responsive Soft Robots Enabled by Self-Powered, Highly Extensible, and Highly Sensitive Triboelectric Proximity- and Pressure-Sensing Skins, Advanced Materials 30 (28) (2018) 1801114, doi:10.1002/adma.201801114.

[21] A. Georgopoulou, F. Clemens, Piezoresistive Elastomer-Based Composite Strain Sensors and Their Applications, ACS Applied Electronic Materials 2 (7) (2020-07-28) 1826–1842, doi:10.1021/acsaelm.0c00278.

[22] N. Lu, D.-H. Kim, Flexible and Stretchable Electronics Paving the Way for Soft Robotics, Soft Robotics 1 (1) (2014-03) 53–62, doi:10.1089/soro.2013.0005.

[23] A. Georgopoulou, B. Vanderborght, F. Clemens, Fabrication of a soft robotic gripper with integrated strain sensing elements using multi-material additive manufacturing, Frontiers in Robotics and AI 8 (2021). https://www.frontiersin.org/article/10.3389/frobt.2021.615991

[24] J. Kang, J.B.-H. Tok, Z. Bao, Self-healing soft electronics, Nature Electronics 2 (4) (2019-04) 144–150, doi:10.1038/s41928-019-0235-0.

[25] E. Roels, S. Terryn, J. Brancart, G.V. Assche, B. Vanderborght, A Multi-Material Self-Healing Soft Gripper, in: 2019 2nd IEEE International Conference on Soft Robotics (RoboSoft), 2019-04, pp. 316–321, doi:10.1109/ROBOSOFT.2019.8722781.

[26] S. Terryn, E. Roels, J. Brancart, G. Van Assche, B. Vanderborght, Self-Healing and High Interfacial Strength in Multi-Material Soft Pneumatic Robots via Reversible Diels-Alder Bonds, Actuators 9 (2) (2020) 34, doi:10.3390/act9020034.

[27] C. Mattmann, F. Clemens, G. Tröster, Sensor for Measuring Strain in Textile, Sensors 8 (6) (2008-06-03) 3719–3732, doi:10.3390/s8063719.

[28] A. Georgopoulou, S. Michel, B. Vanderborght, F. Clemens, Piezoresistive sensor fiber composites based on silicone elastomers for the monitoring of the position of a robot arm, Sensors and Actuators A: Physical 318 (2021-02-01) 112433, doi:10.1016/j.sna.2020.112433.

[29] D.J. Cohen, D. Mitra, K. Peterson, M.M. Maharbiz, A Highly Elastic, Capacitive Strain Gauge Based on Percolating Nanotube Networks, Nano Letters 12 (4) (2012-04-11) 1821–1825, doi:10.1021/nl204052z.

[30] T. Giffney, M. Xie, A. Yong, A. Wong, P. Mousset, A. McDaid, K. Aw, Soft Pneumatic Bending Actuator with Integrated Carbon Nanotube Displacement Sensor, Robotics 5 (1) (2016-02-24) 7, doi:10.3390/robotics5010007.

[31] F. Orozco, M. Kaveh, D.S. Santosa, G.M.R. Lima, D.R. Gomes, Y. Pei, R. Araya-Hermosilla, I. Moreno-Villoslada, F. Picchioni, R.K. Bose, Electroactive Self-Healing Shape Memory Polymer Composites Based on Diels-Alder Chemistry, ACS Applied Polymer Materials 3 (12) (2021-12-10) 6147–6156, doi:10.1021/acsapm.1c00999.

[32] M. Amjadi, A. Pichitpajongkit, S. Lee, S. Ryu, I. Park, Highly Stretchable and Sensitive Strain Sensor Based on Silver Nanowire-Elastomer Nanocomposite, ACS Nano 8 (5) (2014-05-27) 5154–5163, doi:10.1021/nn501204t.

[33] Z. Zou, C. Zhu, Y. Li, X. Lei, W. Zhang, J. Xiao, Rehealable, fully recyclable, and malleable electronic skin enabled by dynamic covalent thermoset nanocomposite, Science Advances 4 (2) (2018-02) eaaq0508, doi:10.1126/sciadv.aaq0508.

[34] E.J. Markvicka, M.D. Bartlett, X. Huang, C. Majidi, An autonomously electrically self-healing liquid metal–elastomer composite for robust soft-matter robotics and electronics, Nature Materials 17 (7) (2018-07) 618–624, doi:10.1038/s41563-018-0084-7.

[35] M.D. Dickey, Stretchable and Soft Electronics using Liquid Metals, Advanced Materials 29 (27) (2017-07) 1606425, doi:10.1002/adma.201606425.

[36] S.-H. Shin, W. Lee, S.-M. Kim, M. Lee, J.M. Koo, S.Y. Hwang, D.X. Oh, J. Park, Ion-conductive self-healing hydrogels based on an interpenetrating polymer network for a multimodal sensor, Chemical Engineering Journal 371 (2019-09) 452–460, doi:10.1016/j.cej.2019.04.077.

[37] Z. Lei, Q. Wang, S. Sun, W. Zhu, P. Wu, A Bioinspired Mineral Hydrogel as a Self-Healable, Mechanically Adaptable Ionic Skin for Highly Sensitive Pressure Sensing, Advanced Materials 29 (22) (2017) 1700321, doi:10.1002/adma.201700321.

[38] R.L. Truby, M. Wehner, A.K. Grosskopf, D.M. Vogt, S.G.M. Uzel, R.J. Wood, J.A. Lewis, Soft Somatosensitive Actuators via Embedded 3D Printing, Advanced Materials (Deerfield Beach, Fla.) 30 (15) (2018-04) e1706383, doi:10.1002/adma.201706383.

[39] J.Y. Oh, D. Son, T. Katsumata, Y. Lee, Y. Kim, J. Lopez, H.-C. Wu, J. Kang, J. Park, X. Gu, J. Mun, N.G.-J. Wang, Y. Yin, W. Cai, Y. Yun, J.B.-H. Tok, Z. Bao, Stretchable self-healable semiconducting polymer film for active-matrix strain-sensing array, Science Advances 5 (11) (2019-11) eaav3097, doi:10.1126/sciadv.aav3097.

[40] D. Jiang, Y. Wang, B. Li, C. Sun, Z. Wu, H. Yan, L. Xing, S. Qi, Y. Li, H. Liu, W. Xie, X. Wang, T. Ding, Z. Guo, Flexible Sandwich Structural Strain Sensor Based on Silver Nanowires Decorated with Self-Healing Substrate, Macromolecular Materials and Engineering 304 (7) (2019) 1900074, doi:10.1002/mame.201900074.

[41] H. Guo, Y.J. Tan, G. Chen, Z. Wang, G.J. Susanto, H.H. See, Z. Yang, Z.W. Lim, L. Yang, B.C.K. Tee, Artificially innervated self-healing foams as synthetic piezo-impedance sensor skins, Nature Communications 11 (1) (2020-11-12) 5747, doi:10.1038/s41467-020-19531-0.

[42] A. Rana, J.-P. Roberge, V. Duchaine, An Improved Soft Dielectric for a Highly Sensitive Capacitive Tactile Sensor, IEEE Sensors Journal 16 (22) (2016-11) 7853–7863, doi:10.1109/JSEN.2016.2605134.

[43] M. Saari, B. Xia, B. Cox, P.S. Krueger, A.L. Cohen, E. Richer, Fabrication and Analysis of a Composite 3D Printed Capacitive Force Sensor, 3D Printing and Additive Manufacturing 3 (3) (2016-09-01) 136–141, doi:10.1089/3dp.2016.0021.

[44] M. Khatib, O. Zohar, H. Haick, Self-Healing Soft Sensors: From Material Design to Implementation, Advanced Materials 33 (11) (2021) 2004190, doi:10.1002/adma.202004190.

[45] A. Cuvellier, R. Verhelle, J. Brancart, B. Vanderborght, G. Van Assche, H. Rahier, The influence of stereochemistry on the reactivity of the Diels–Alder cycloaddition and the implications for reversible network polymerization, Polymer Chemistry 10 (4) (2019) 473–485, doi:10.1039/C8PY01216D.

[46] S. Terryn, J. Brancart, E. Roels, R. Verhelle, A. Safaei, A. Cuvellier, B. Vanderborght, G. Van Assche, Structure-property relationships of Diels-Alder-based reversible crosslinked networks for self-healing soft robots, in press (2022).

[47] L. Flandin, A. Hiltner, E. Baer, Interrelationships between electrical and mechanical properties of a carbon black-filled ethylene–octene elastomer, Polymer 42 (2) (2001-01) 827–838, doi:10.1016/S0032-3861(00)00324-4.

[48] N. Hu, Y. Karube, C. Yan, Z. Masuda, H. Fukunaga, Tunneling effect in a polymer/carbon nanotube nanocomposite strain sensor, Acta Materialia 56 (13) (2008-08-01) 2929–2936, doi:10.1016/j.actamat.2008.02.030.

[49] K.C. Etika, L. Liu, L.A. Hess, J.C. Grunlan, The influence of synergistic stabilization of carbon black and clay on the electrical and mechanical properties of epoxy composites, Carbon 47 (13) (2009-11-01) 3128–3136, doi:10.1016/j.carbon.2009.07.031.

[50] A. Georgopoulou, C. Kummerlöwe, F. Clemens, Effect of the Elastomer Matrix on Thermoplastic Elastomer-Based Strain Sensor Fiber Composites, Sensors 20 (8) (2020-04-23) 2399, doi:10.3390/s20082399.

[51] A. Georgopoulou, A.W. Bosman, J. Brancart, B. Vanderborght, F. Clemens, Supramolecular Self-Healing Sensor Fiber Composites for Damage Detection in Piezoresistive Electronic Skin for Soft Robots, Polymers 13 (17) (2021-01) 2983, doi:10.3390/polym13172983.

[52] M. Melnykowycz, B. Koll, D. Scharf, F. Clemens, Comparison of piezoresistive monofilament polymer sensors, Sensors (Basel, Switzerland) 14 (1) (2014-01-13) 1278–1294, doi:10.3390/s140101278.

[53] M. Amjadi, K.-U. Kyung, I. Park, M. Sitti, Stretchable, Skin-Mountable, and Wearable Strain Sensors and Their Potential Applications: A Review, Advanced Functional Materials 26 (11) (2016-03) 1678–1698, doi:10.1002/adfm.201504755.

[54] M. Ottenio, D. Tran, A. Ní Annaidh, M.D. Gilchrist, K. Bruyère, Strain rate and anisotropy effects on the tensile failure characteristics of human skin, Journal of the Mechanical Behavior of Biomedical Materials 41 (2015-01) 241–250, doi:10.1016/j.jmbbm.2014.10.006.

[55] J.T. Muth, D.M. Vogt, R.L. Truby, Y. Mengüç, D.B. Kolesky, R.J. Wood, J.A. Lewis, Embedded 3D Printing of Strain Sensors within Highly Stretchable Elastomers, Advanced Materials 26 (36) (2014-09) 6307–6312, doi:10.1002/adma.201400334.

[56] D.S.A.D. Focatiis, D. Hull, A. Sánchez-Valencia, Roles of prestrain and hysteresis on piezoresistance in conductive elastomers for strain sensor applications, Plastics, Rubber and Composites 41 (7) (2012-09-01) 301–309, doi:10.1179/1743289812Y.0000000022.

[57] J. Shintake, E. Piskarev, S.H. Jeong, D. Floreano, Ultrastretchable Strain Sensors Using Carbon Black-Filled Elastomer Composites and Comparison of Capacitive Versus Resistive Sensors, Advanced Materials Technologies 3 (3) (2018) 1700284, doi:10.1002/admt.201700284.

[58] B. Oldfrey, R. Jackson, P. Smitham, M. Miodownik, A Deep Learning Approach to Non-linearity in Wearable Stretch Sensors, Frontiers in Robotics and AI 6 (2019), doi:10.3389/frobt.2019.00027.

[59] B. Shih, D. Shah, J. Li, T.G. Thuruthel, Y.-L. Park, F. Iida, Z. Bao, R. Kramer-Bottiglio, M.T. Tolley, Electronic skins and machine learning for intelligent soft robots, Science Robotics (2020-04-22), doi:10.1126/scirobotics.aaz9239.

[60] L. Viry, A. Levi, M. Totaro, A. Mondini, V. Mattoli, B. Mazzolai, L. Beccai, Flexible Three-Axial Force Sensor for Soft and Highly Sensitive Artificial Touch, Advanced Materials 26 (17) (2014) 2659–2664, doi:10.1002/adma.201305064.